ELSEVIER

Effect of an exponentially decaying threshold on the firing statistics of a stochastic integrate-and-fire neuron

Benjamin Lindner*, André Longtin

Department of Physics, University of Ottawa, 150 Louis Pasteur, Ont., Ottawa, Canada KIN 6N5

Abstract

We study a white-noise driven integrate-and-fire (IF) neuron with a time-dependent threshold. We give analytical expressions for mean and variance of the interspike interval assuming that the modification of the threshold value is small. It is shown that the variability of the interval can become both smaller or larger than in the case of constant threshold depending on the decay rate of threshold. We also show that the relative variability is minimal for a certain finite decay rate of the threshold. Furthermore, for slow threshold decay the leaky IF model shows a minimum in the coefficient of variation whenever the firing rate of the neuron matches the decay rate of the threshold. This novel effect can be seen if the firing rate is changed by varying the noise intensity or the mean input current.
© 2004 Elsevier Ltd. All rights reserved.

1. Introduction

Integrate-and-fire (IF) models are nowadays frequently used to understand generic effects in neural signal transmission or network behavior. Compared to more realistic multidimensional ionic models, IF neurons can be easily used in large network simulations; they also permit in many instances an analytical approach to diverse problems like, for instance, spike train variability, neural signal transmission, or network oscillations.

Stochastic IF models that take into account random influences (channel noise, random synaptic input, etc.) have a long history and are still used frequently for modeling purposes. The "standard" system for this kind of modeling is a perfect or leaky IF neuron driven by an input current and a white Gaussian background noise

(for reviews, see Ricciardi and Sacerdote, 1979; Tuckwell, 1988; Lánský and Rospars, 1995). Recent research has focused on analytical approaches for extensions of this basic model by taking into account a finite correlation time of the input noise (Fourcaud and Brunel, 2002; Middleton et al., 2003; Lindner, 2004a) or the inclusion of a nonlinear leakage term (quadratic IF model) (Gutkin and Ermentrout, 1998; Lindner et al., 2003; Brunel and Latham, 2003) that corresponds to a type I neuronal dynamics (Ermentrout, 1996; Gutkin and Ermentrout, 1998).

Another extension that has been used in a number of studies is an IF model with a time-dependent threshold (Tuckwell, 1978; Vasudevan and Vittal, 1982; Wilbur and Rinzel, 1983; Tuckwell and Wan, 1984; Rappel and Karma, 1996; Chacron et al., 2000, 2001, 2003) (see also Holden, 1976, Chapter 4 for further references). Such models have been considered for several reasons. A decaying threshold, for instance, mimics the effect of an afterhyperpolarization observed in many neurons. More generally, it may be looked upon as a mechanism for a relative refractory period. Recent interest in IF models

*Corresponding author. Tel.: +1 613 562 5800;
fax: +1 613 562 5190.

E-mail address: lindner.benjamin@science.uottawa.ca
(B. Lindner).

with a time-dependent threshold originates in the study of *non-renewal* spike trains: if the threshold obeys a dynamics driven by the spikes of the IF model, negative ISI correlations can be observed. In particular, a leaky IF model with a dynamical threshold (LIFDT model) has been used to reproduce with high accuracy the firing statistics of electrosensory neurons (Chacron et al., 2000, 2001).

Here we consider a white-noise driven IF model with exponentially decaying threshold as used by Tuckwell (1978) and Tuckwell and Wan (1984). The threshold starts after each reset of the voltage at the same fixed value, i.e. this model will generate a renewal process. We focus on the mean, variance, and coefficient of variation (CV) as functions of the system parameters. These statistics are of general interest both for the characterization of the spontaneous neural activity as well as for the neuronal signal transmission. Our study may help to understand under which conditions a decaying threshold may facilitate or deteriorate signal processing by stochastic neurons. Although the considered model generates a renewal process, it is very close to the non-renewal LIFDT model mentioned above and may be regarded as a simplified version of the latter. In this respect our results may also be taken as a first step towards an understanding of the more complicated LIFDT model.

Since IF models with time-dependent threshold pose a complicated first-passage-time (FPT) problem, most of the previous work employed numerical simulations. Tuckwell and Wan (1984) derived a partial differential equation governing the ISI moments; these equations, however, were solved numerically. For the case of a perfect IF model driven by Poissonian shot noise with a certain amplitude distribution, Vasudevan and Vittal (1982) gave implicit relations for the ISI density; a numerical evaluation of those relations were not performed in this work, though. Researchers in the field of applied probability theory focused on the asymptotic behavior (i.e. the tail) of the FPT density (Giorno et al., 1990) and on specific threshold functions where the FPT density can be exactly solved (Jáimez et al., 1995; Gutiérrez et al., 1997); the latter do not include the specific problem considered here. In this paper, we give explicit expressions for mean and variance of the ISI in the presence of an exponentially decaying threshold. Our results hold true for the entire range of decay rates of the threshold but require the threshold modulation to be weak. The theory relies on very recent results for the FPT problem in the presence of a time-dependent drift derived by one of the authors (Lindner, 2004b).

Our results show that for either perfect and leaky IF models, there exists an optimal decay rate that minimizes the relative variability; i.e. the CV plotted as a function of the decay rate passes through a minimum. In particular for a leaky IF model, the relative

variability can be either larger or smaller than in the case of a constant threshold. Further, the firing rate is in general diminished by the time-dependence of the threshold. All of these effects, however, are rather small as long as the amplitude of the time-dependent change in threshold is small ($<20\%$ of the unperturbed constant threshold). An exception to this is a novel effect found at slow threshold decay for the leaky IF model operating in a Poissonian firing regime. Here the relative variability shows a minimum as a function of either mean input current or noise intensity; the minimum occurs at parameter sets for which the firing rate of the neuron roughly equals the decay rate of the threshold. The minimum can be rather pronounced already for a small amplitude of the threshold decay. We note that a minimum in the CV as a function of the firing rate was observed experimentally in nerve afferents of the squirrel monkey (Goldberg et al., 1984) and also obtained by numerical simulations of an IF model with AHP current (Smith and Goldberg, 1986).

This paper is organized as follows. In Section 2, we introduce the model and the quantities of interest; we also give a description of the integration procedure for the numerical simulation of the first-passage process. In Section 3, we present the analytical results for the mean and variance of the ISI in the presence of a decaying threshold. In Section 4, the effect of the decaying threshold on mean, variance, and coefficient of variation is explored; we shall consider the functional dependences of these statistics on the various system parameters (decay rate, base current, noise intensity) and compare some of our analytical findings to results of numerical simulations. In Section 5, we summarize our findings and discuss briefly their neurobiological implications.

2. The Models and their numerical simulation

We consider an IF model driven by a constant base current μ and a white Gaussian noise $\xi(t)$ with intensity parameter σ that obeys the stochastic differential equation of an Ornstein–Uhlenbeck process

$$\dot{v} = -\alpha v + \mu + \sigma\xi(t). \tag{1}$$

Time is measured in multiples of the membrane time constant τ_{mem}. The base current and the noise intensity differ only by scalar factors from the parameters of a noisy input current as, for instance, used in an experiment in vitro. The above equation has still to be complemented by a spike-and-reset rule. Whenever the voltage v reaches the threshold value Θ, a spike is fired and the variable v is reset to $v = v_R = 0$. The interspike intervals (ISIs) are then the first passage times of the variable v from $v = 0$ to $v = \Theta(t)$. The common way to

incorporate an absolute refractory period is to add a constant time τ_{abs} to the first passage time. For the sake of simplicity, we set here $\tau_{abs} = 0$. For the standard leaky IF model, we set $\alpha = 1$ without loss of generality. The case of negligible leakage (perfect IF model) corresponds to $\alpha = 0$. In both cases, Θ is usually a constant that can be normalized to one. Here we consider as was done by Tuckwell (1978) a time-dependent threshold that introduces an additional relative refractory period. In particular we have

$$\Theta(t) = 1 + \varepsilon \exp[-\lambda(t - t_k)], \qquad (2)$$

where t_k is the last spiking time and λ is referred to as the decay rate of the threshold. The model is illustrated for $\alpha = 1$ and a slow decay rate in Fig. 1, showing the time courses of the voltage variable and of the threshold; spikes and one ISI are also indicated.

It is important to note that this IF model still generates a renewal spike train, i.e. there are no correlations among the ISIs generated by the IF neuron. The effect of the time-dependent threshold is therefore restricted to the statistics of the single ISI henceforth denoted by T. Here we consider the most important characteristics of the single ISI: its mean $\langle T \rangle$ and its variability. Since often the stationary firing rate is measured instead of the mean ISI, we may also consider the rate given by

$$r = \frac{1}{\langle T \rangle}. \qquad (3)$$

The variability can be quantified either by the variance

$$\langle \Delta T^2 \rangle = \langle T^2 \rangle - \langle T \rangle^2 \qquad (4)$$

and by the standard deviation $\sqrt{\langle \Delta T^2 \rangle}$ of the ISI or by a relative measure like the coefficient of variation (CV)

that compares the fluctuations in the ISI (its standard deviation) to the mean ISI

$$CV = \frac{\sqrt{\langle \Delta T^2 \rangle}}{\langle T \rangle}. \qquad (5)$$

First we discuss some simple limits of the model and what kind of effects of the time-dependent threshold might be intuitively expected in general.

If $\lambda = 0$ or very small, the model functions like a standard IF model with rescaled *constant* threshold $\Theta = 1 + \varepsilon$. For $\lambda \to \infty$ in turn we expect that the threshold quickly approaches $\Theta = 1$ and hence the behavior of the model will be exactly that for $\varepsilon = 0$. For arbitrary λ the mean ISI can be expected to always be larger than in the case of constant threshold with $\varepsilon = 0$. Evidently, each realization reaching $\Theta(t) = 1 + \varepsilon e^{-\lambda(t-t_k)}$ must have exceeded $v = 1$, thus for each realization, the first passage time will be larger than in the unperturbed case $\varepsilon = 0$.

It is not clear at the first glance, however, what is going to happen to the absolute and relative *variability* of the ISI measured by variance and CV, respectively. Thinking of the decaying threshold as a refractory mechanism, one might be tempted to conclude that the relative variability will always be lower than for a constant threshold. Furthermore it may be of interest with regard to signal transmission properties of the IF model whether the ISI variability can be minimized. These issues will be clarified by means of the analytical results that are derived in the next section. Before we come to the analytical treatment, we will discuss briefly the numerical simulation of the first passage time problem.

2.1. Numerical simulations of the stochastic differential equations

In order to measure the statistics of the ISI, one may employ a numerical simulation of the model. In practice, this means to approximate the integration of Eq. (1) with a difference scheme for the voltage $v_i = v(t_i)$ at discrete times $t_i = i\Delta t$ where Δt is the time step. Starting at $i = 0$ with $v_0 = v_R = 0$, one may use an Euler procedure with an appropriate scaling of the noise term (Risken, 1984)

$$v_{i+1} = v_i + (\mu - \alpha v_i)\Delta t + \sigma\sqrt{\Delta t}\xi_i, \qquad (6)$$

where the ξ_i are independent zero-mean Gaussian random numbers with unit variance. The simulation is performed until for the first time $v_{i+1} > \Theta(t_{i+1})$ (this has to be checked at every time step) which gives us the first stochastic realization of the ISI

$$T_1 \approx (i + 1/2)\Delta t. \qquad (7)$$

Starting again at $i = 0$ with $v_0 = 0$ and repeating this procedure many times (a typical value is $N = 10^6$)
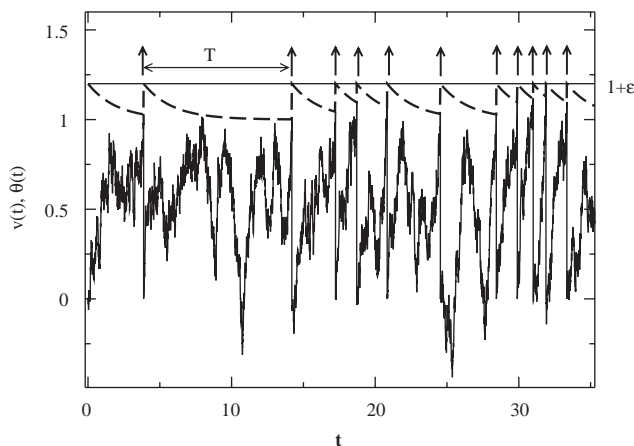

Fig. 1. The trajectory of the leaky IF model with exponentially decaying threshold. The time course of the threshold (restarted after each firing at $1 + \varepsilon$) is shown by the dashed line, arrows represent spikes and one ISI is explicitly indicated. Parameters are $\mu = 0.8$, $\sigma^2 = 0.2$, $\lambda = 0.5$, and $\varepsilon = 0.2$.

allows the determination of the ISI's mean and variance with sufficient accuracy. The mean, for instance, is given by the sum over all realizations of the ISI

$$\langle T \rangle = \frac{1}{N} \sum_{j=1}^{N} T_j. \tag{8}$$

By approximating the stochastic differential equation with the difference scheme Eq. (6), we may make, though, an error in estimating the ISI. First of all, it is clear that if $v_{i+1} > \Theta(t_{i+1})$ we cannot tell at which time within the interval $[t_i, t_{i+1}]$ the threshold has been crossed, thus, the ISI is only determined with an uncertainty of order of magnitude Δt. We may decrease the time step (thus increasing, of course, the computation time) in order to reduce this error. For the perfect IF model, a time step of $\Delta t = 10^{-3}$ was sufficient to reproduce with the desired accuracy mean and variance with constant threshold for which we know the exact results for these quantities. We employed the above procedure to estimate mean and variance of the ISI for the perfect IF dynamics with time dependent threshold using at each data point 10^6 ISIs.

There is, however, an additional systematic error made in estimating the interval. This error seemed to be more severe for the leaky IF model than for the perfect IF model. Even if both v_i and v_{i+1} are smaller than the value of the time-dependent threshold, the voltage could have exceeded the threshold in between t_i and t_{i+1}. This introduces a systematic error (an overestimation of the ISI) in proportion to the square root of the time step and thus results in a very slow convergence of the numerical procedure when the time step is decreased. A linear convergence can be restored by accepting a successful passage with the interval $[t_i, t_{i+1}]$ for subthreshold values $v(t_i), v(t_{i+1}) < V_T$ with finite probability (cf. Honerkamp, 1993)

$$P(v_i, v_{i+1})$$
$$= \exp \left[2 \frac{(v_i + v_{i+1})V_T - v_i v_{i+1} - V_T^2}{\sigma^2 \Delta t} \right], \tag{9}$$

where in our case we took the threshold value V_T to be equal to the time dependent threshold at $t = t_{i+1}$, i.e. $V_T = \Theta(t_{i+1})$.

The actual implementation of the numerical algorithm is as follows. We employed the finite difference scheme until v_i crossed a predefined subthreshold value (typically, 80–90% of the lower limit of $\Theta(t)$; for values v_i, v_{i+1} below this the crossing probability Eq. (9) is exponentially small). After this event we continued with Eq. (6) but also drew a uniform random number a_i. For both events where either $v_{i+1} > \Theta(t_{i+1})$ *or* where we had $a_i < P(v_i, v_{i+1}, \Theta(t_{i+1}))$ for subthreshold values v_i, v_{i+1}, a spike is said to have occurred and we set $T = (i + 1/2)\Delta t$; otherwise the simulation was continued. Using this scheme for the leaky IF model, simulations with

$\Delta t = 10^{-2}$ led to satisfying agreement with exact analytical results for $\varepsilon = 0$. We also checked the convergence with decreasing time step for two different parameter sets and confirmed that $\Delta t = 10^{-2}$ achieved the desired numerical accuracy. For each data set (except for Fig. 13, see Figure caption), 10^6 ISIs were used in order to determine the ISI's mean and variance. We want to point out that these simulations can be rather time-consuming, in particular, if an accuracy of one percent or less is required. Of course, one may get a rough impression of the model by a short simulation with poor statistics; doing so, one may, however, miss important features of the neuronal dynamics. In this light, it seems to be worth to invest some time and efforts to derive analytical approximations for the ISI statistics.

3. Theory

The dynamics Eq. (1) with the exponentially decaying threshold Eq. (2) can be easily transformed to an IF model with constant threshold but time-dependent drift. This transformation is given by

$$\tilde{v} = \frac{v - \varepsilon e^{-\lambda t} + \varepsilon}{1 + \varepsilon}. \tag{10}$$

For both perfect and leaky IF models this transformation yields an exponentially decaying drift and rescaled parameters μ, σ, and ε.

The general problem of a time-dependent drift has been recently addressed by a novel analytical approach in Lindner (2004b). In that paper general relations for the linear corrections to the moments of the first-passage time in the presence of a time-dependent drift were given. Starting from the Fokker–Planck equation governing the probability density of the first-passage process, a perturbation approach yielded the first correction terms (i.e. the term proportional to the amplitude of the time-dependent drift) to each moment of the first-passage time expressed by quadratures of the probability density in the absence of the time-dependent drift. Explicit formulas were derived for the cases of a linear potential (i.e. a biased random walk) and a parabolic potential both with an exponentially decaying force of the form $\lambda e^{-\lambda t}$. These cases correspond to the dynamics of the perfect and leaky IF model with exponentially decaying drift, respectively, i.e. to the models that are obtained from those considered here if we apply the transformation Eq. (10).

Since we can map the problem of an IF model with time-dependent threshold to the solved problem of an IF model with time-dependent drift, it appears sufficient to adopt the respective formulas for mean and variance given by Lindner (2004b). This is indeed possible for the perfect IF model. However, for the leaky IF model, a

closer inspection reveals that additional efforts have to be made to achieve formulas for mean and variance that hold true for a large range of decay rates. The reason for this is that the transformation Eq. (10) yields also a rescaling of parameters such that the time-dependent driving is not the same as considered by Lindner (2004b).

In the following, we derive mean and variance of the ISI for a perfect IF model ($\alpha = 0$) and for a leaky IF model ($\alpha = 1$) separately; rate and CV can then be easily determined using Eqs. (3) and (5).

3.1. Theory for the perfect integrator

For $\alpha = 0$, the transformation Eq. (10) yields the following dynamics for the new variable $\tilde{v}$

$$\dot{\tilde{v}} = \tilde{\mu} + \tilde{\varepsilon}\lambda e^{-\lambda t} + \tilde{\sigma}\xi(t) \qquad (11)$$

with threshold at $\tilde{v}_T = 1$ and reset to $\tilde{v}_R = 0$ after firing. It might be surprising that the decaying threshold acts like an *excitatory* driving in a perfect IF model with constant threshold. Note, however, that also the parameters of the system (μ, D, and ε) have been rescaled as follows:

$$\tilde{\mu} = \frac{\mu}{1 + \varepsilon}, \quad \tilde{\varepsilon} = \frac{\varepsilon}{1 + \varepsilon}, \quad \tilde{\sigma} = \frac{\sigma}{(1 + \varepsilon)}, \qquad (12)$$

i.e., the base current and noise intensity have been reduced.

The first passage time problem for a dynamics Eq. (11) has been treated by a perturbation method in Lindner (2004b); the resulting formulas for the mean and the variance read in our notation

$$\langle T \rangle = \frac{1}{\tilde{\mu}} - \frac{\tilde{\varepsilon}}{\tilde{\mu}}\left(1 - \exp\left[\frac{\tilde{\mu} - \sqrt{\tilde{\mu}^2 + 2\lambda\tilde{\sigma}^2}}{\tilde{\sigma}^2}\right]\right), \qquad (13)$$

$$\langle \Delta T^2 \rangle = \tilde{\sigma}^2 \frac{1 - \tilde{\varepsilon}}{\tilde{\mu}^3} + \frac{2\tilde{\varepsilon}}{\tilde{\mu}^2}\left(\frac{\tilde{\mu}}{\sqrt{\tilde{\mu}^2 + 2\lambda\tilde{\sigma}^2}} + \frac{\tilde{\sigma}^2}{2\tilde{\mu}} - 1\right)$$
$$\times \exp\left[\frac{\tilde{\mu} - \sqrt{\tilde{\mu}^2 + 2\lambda\tilde{\sigma}^2}}{\tilde{\sigma}^2}\right]. \qquad (14)$$

Using the original parameters via Eq. (12) and taking into account only constant and linear terms in ε leads to the following formulas for a perfect IF model with an exponentially decaying threshold

$$\langle T \rangle = \frac{1}{\mu} + \frac{\varepsilon}{\mu}\exp\left[\frac{\mu - \sqrt{\mu^2 + 2\lambda\sigma^2}}{\sigma^2}\right], \qquad (15)$$

$$\langle \Delta T^2 \rangle = \frac{\sigma^2}{\mu^3} + \frac{2\varepsilon}{\mu^2}\left(\frac{\mu}{\sqrt{\mu^2 + 2\lambda\sigma^2}} + \frac{\sigma^2}{2\mu} - 1\right)$$
$$\times \exp\left[\frac{\mu - \sqrt{\mu^2 + 2\lambda\sigma^2}}{\sigma^2}\right]. \qquad (16)$$

It is readily seen that Eqs. (15) and (16) differ from Eqs. (13) and (14) only by a constant. The implications of this constant are, however, important: a positive exponential driving will always lead to a decrease in mean and variance of the first-passage time (cf. the discussion of these issues in (Lindner, 2004b)) while quite to the contrary a decaying threshold leads to a longer mean first-passage time (i.e. mean ISI) than for $\varepsilon = 0$.

Let us start with some general observations regarding the formulas Eqs. (15) and (16).

As already mentioned, for positive ε (as assumed throughout the following), the mean ISI Eq. (15) increases compared to the unperturbed case ($\varepsilon = 0$) which makes sense and is in accordance with our remarks in the introduction of the model. The correction to the variance, however, may change sign: for low λ the prefactor of the exponential is evidently positive while for large λ it will be negative if the noise is not too strong ($\sigma \ll \mu$). For $\varepsilon = 0$ or for $\lambda \to \infty$ the formulas yield the well-known results for a white-noise driven perfect IF model with constant threshold

$$\langle T \rangle_0 = \frac{1}{\mu}, \qquad (17)$$

$$\langle \Delta T^2 \rangle_0 = \frac{\sigma^2}{\mu^3}, \qquad (18)$$

where the index "0" indicates that $\varepsilon = 0$. For $\lambda = 0$ we find

$$\langle T \rangle_{\lambda=0} = \frac{1 + \varepsilon}{\mu}, \qquad (19)$$

$$\langle \Delta T^2 \rangle_{\lambda=0} = \frac{\sigma^2(1 + \varepsilon)}{\mu^3}, \qquad (20)$$

which also corresponds to the white-noise driven perfect IF model but with a reset-threshold distance of $1 + \varepsilon$.

Further, for vanishing noise $\sigma = 0$, the ISI of the deterministic system T_{det} can be calculated for arbitrary amplitude ε

$$T_{det} = \frac{1}{\mu} + \frac{1}{\lambda}\,\mathrm{LW}(\varepsilon e^{-\lambda/\mu}\lambda/\mu)$$
$$= \frac{1}{\mu} + \frac{\varepsilon}{\mu}e^{-\lambda/\mu} - \frac{\varepsilon^2\lambda}{\mu^2}\,e^{-2\lambda/\mu} + \cdots, \qquad (21)$$

where $\mathrm{LW}(x)$ is the Lambert W function.[1] In the second line of Eq. (21), we give the first three terms of a Taylor expansion. Remarkably, up to first order in ε this is the same as we obtain from Eq. (15) for $\sigma = 0$, i.e. the term linear in ε equals the perturbation correction from

---

[1]In the absence of noise, the ISI is determined by the intersection of threshold $\Theta(T) = 1 + \varepsilon e^{-\lambda T}$ and the deterministic passage of the voltage $v(T) = \mu T$. This equation can be brought into the form $\mathrm{LW}(x) * \exp[\mathrm{W}(x)] = x$ with $x = \varepsilon e^{-\lambda/\mu}\lambda/\mu$ that is solved by the real branch of the Lambert W function for $x > 0$ (Corless et al., 1996).

Eq. (15) at $\sigma = 0$, implying that the latter is valid in the weak noise limit. Note that the variance of the ISI has to be zero in the case of $\sigma = 0$ for obvious reasons.

3.2. Theory for the leaky integrator

For a leaky IF model ($\alpha = 1$), the variable transformation Eq. (10) now leads to the dynamics

$$\dot{\tilde{v}} = -\tilde{v} + \frac{\varepsilon}{1+\varepsilon}(\lambda - 1)e^{-\lambda t} + \frac{\varepsilon}{1+\varepsilon} + \frac{\mu}{1+\varepsilon}$$
$$+ \frac{\sigma}{1+\varepsilon}\,\xi(t). \tag{22}$$

Interestingly, the dynamics includes an exponentially decaying drift term with amplitude proportional to ($\lambda - 1$). From this, one can conclude that the problem is exactly solvable not only for $\lambda \to 0$ and $\lambda \to \infty$ but also for $\lambda = 1$ since in this case the time dependent driving vanishes and we obtain the standard white-noise driven leaky IF model with constant, though rescaled parameters. We will use this fact later on.

For arbitrary values of λ, we can again profit from (Lindner, 2004b). There it was shown that for the process

$$\dot{x} = -bx + a + \varepsilon\lambda e^{-\lambda t} + \sqrt{2D}\xi(t) \tag{23}$$

with small ε the mean and variance of the passage time from 0 to x_E can be expressed by

$$\langle T \rangle = \langle T \rangle_0 + \varepsilon\delta_1(\lambda), \tag{24}$$

$$\langle \Delta T^2 \rangle = \langle \Delta T^2 \rangle_0 + \varepsilon\delta_2(\lambda), \tag{25}$$

where $\langle T \rangle_0$ and $\langle \Delta T^2 \rangle_0$ are the mean and variance in the case of $\varepsilon = 0$ and δ_1, δ_2 are the linear corrections due to the presence of the time-dependent drift. The former functions can be written as follows (Lindner et al., 2002)

$$\langle T \rangle_0 = \frac{\sqrt{\pi}}{b} \int_{x_-}^{x_+} dy\, e^{y^2} \mathrm{erfc}(y), \tag{26}$$

$$\langle \Delta T^2 \rangle_0 = \frac{2\pi}{b^2} \int_{x_-}^{\infty} dy\, e^{y^2} [\mathrm{erfc}(y)]^2$$
$$\times \int_{x_-}^{y} dz\, e^{z^2} H(x_+ - z), \tag{27}$$

where we have used the Heaviside function $H(x)$ (Abramowitz and Stegun, 1970) and the abbreviations

$$x_- = \frac{a - bx_E}{\sqrt{2Db}}, \quad x_+ = \frac{a}{\sqrt{2Db}}. \tag{28}$$

The correction terms are given by

$$\delta_1(\lambda) = \frac{\lambda}{\lambda - b}\sqrt{\frac{\pi}{2bD}}e^{x_+^2}[e^{\delta}\rho_0(\lambda)\mathrm{erfc}(x_-)$$
$$- \mathrm{erfc}(x_+)] \tag{29}$$

$$\delta_2(\lambda) = -\frac{\lambda}{\lambda - b}\sqrt{\frac{2\pi}{Db}}e^{x_+^2}\big[e^{\delta}\mathrm{erfc}(x_-)[\rho_0'(\lambda)$$
$$+ \langle T \rangle_0\rho_0(\lambda)]$$
$$+ \frac{\sqrt{\pi}}{b}\int_{x_-}^{\infty} dx\, e^{x^2}\mathrm{erfc}^2(x)[H(x - x_+)$$
$$- e^{\delta}\rho_0(\lambda)]\big], \tag{30}$$

where we have used the Laplace transform of the ISI density of the unperturbed ($\varepsilon = 0$) system $\rho_0(\lambda)$ and its derivative with respect to λ, denoted by $\rho_0'(\lambda)$. The function $\rho_0(\lambda)$ can be expressed by the parabolic cylinder function $\mathscr{D}_a(z)$ (Abramowitz and Stegun, 1970) as follows (Holden, 1976):

$$\rho_0(\lambda) = e^{-\delta/2}\frac{\mathscr{D}_{-\lambda/b}(x_+\sqrt{2})}{\mathscr{D}_{-\lambda/b}(x_-\sqrt{2})}, \quad \delta = x_-^2 - x_+^2. \tag{31}$$

We can use the formulas given in Eqs. (24) and (25) in a straightforward manner, replacing the amplitude ε by $\varepsilon(\lambda - 1)/[\lambda(1+\varepsilon)]$ and setting

$$b = 1, \quad a = \frac{\mu + \varepsilon}{1+\varepsilon}, \quad D = \frac{\sigma^2}{2(1+\varepsilon)^2}. \tag{32}$$

Explicitly, the mean and variance are then given by

$$\langle T \rangle = \left[\langle T \rangle_0 + \frac{\varepsilon(\lambda - 1)}{\lambda(1+\varepsilon)}\delta_1(\lambda)\right]\Bigg|_{b=1,\,a=(\mu+\varepsilon)/(1+\varepsilon),\,D=\sigma^2/[2(1+\varepsilon)^2]}, \tag{33}$$

$$\langle \Delta T^2 \rangle = \left[\langle \Delta T^2 \rangle_0 + \frac{\varepsilon(\lambda - 1)}{\lambda(1+\varepsilon)}\right.$$
$$\left.\times\delta_2(\lambda)\right]\Bigg|_{b=1,\,a=(\mu+\varepsilon)/(1+\varepsilon),\,D=\sigma^2/[2(1+\varepsilon)^2]}. \tag{34}$$

This will not necessarily work well for all parameter values, though. Consider, for instance, the limit $\lambda \to 0$ in Eq. (22). Obviously, in this case the second and the third term cancel each other and we are left with the leaky IF with constant threshold and constant drift with values of μ and σ rescaled by a factor $1/(1+\varepsilon)$. This, however, is not reflected in Eqs. (33) and (34) where the constant term $\varepsilon/(1+\varepsilon)$ was included in the effective bias term a. A similar discrepancy is encountered in the limit of $\lambda \to \infty$; in fact, the formulas Eqs. (33) and (34) can be expected to work fine only for decay rates that are close to 1, i.e. close to the inverse membrane time constant of the leaky IF model.

A closer inspection of the error made at small λ in Eqs. (33) and (34) reveals that there is an *ambiguity* in the perturbation calculation. Above we have only considered the linear correction of the mean and variance due to a time-dependent drift. Evidently there is also a change in the static parameters of the system due to the transformation Eq. (10). The linear correction

to such a change is given by the derivative of the respective function multiplied by the change in parameter according to a simple Taylor expansion. Instead of lumping the third term in Eq. (22) into the effective base current we could treat it as an static perturbation which is equivalent to expanding the *unperturbed* mean ISI at the effective base current as follows:

$$\langle T\rangle_0\left(\frac{\mu+\varepsilon}{1+\varepsilon}\right) \approx \langle T\rangle\left(\frac{\mu}{1+\varepsilon}\right)$$
$$+ \left.\frac{\partial\langle T\rangle_0(\tilde\mu)}{\partial\tilde\mu}\right|_{\tilde\mu=\mu/(1+\varepsilon)} \frac{\varepsilon}{1+\varepsilon}. \tag{35}$$

In other words, if the base current of the unperturbed system were taken as $\mu/(1+\varepsilon)$, then the linear correction in Eq. (24) would consist of a sum of the corrections due to the time-dependent drift and due to the static change in the drift. This kind of perturbation correction is as justified as that in Eqs. (33) and (34). More generally, the same idea can be also applied to the noise strength σ. The whole procedure becomes more clear by recasting the Langevin Eq. (22) into the form

$$\dot{\tilde v} = -\tilde v + \frac{1}{1+\varepsilon}\left[\varepsilon(\lambda-1)\mathrm{e}^{-\lambda t} + (\mu+c_1\varepsilon)\right.$$
$$\left. + \underline{\varepsilon(1-c_1)} + [\sigma(1+\varepsilon c_2) - \underline{c_2\varepsilon\sigma}]\xi(t)\right]. \tag{36}$$

We have introduced some terms proportional to new undetermined parameters c_1 and c_2. Of course, nothing has changed compared to Eq. (22) since all terms containing c_1 or c_2 cancel out. The crucial point is the way we interpret this equation in the context of the perturbation calculation: besides the correction with respect to the time-dependent drift (that has not changed by introducing c_1 and c_2), we consider also the linear correction with respect to a small change in the static parameters of the system. The static parameters are now given by

$$\hat\mu = \frac{\mu+c_1\varepsilon}{1+\varepsilon}, \quad \hat\sigma = \sigma\frac{1+\varepsilon c_2}{1+\varepsilon}; \tag{37}$$

note that they depend on c_1, c_2 too. The small changes in the static parameters are indicated by the underlined terms in Eq. (36). The linear corrections to mean and variance are then given by

$$\langle T\rangle = \langle T\rangle_0 + \frac{\varepsilon}{1+\varepsilon}\left[\frac{\lambda-1}{\lambda}\delta_1(\lambda) + (1-c_{1,T})\right.$$
$$\left. \times \frac{\partial\langle T\rangle_0}{\partial\hat\mu} - \sigma c_{2,T}\frac{\partial\langle T\rangle_0}{\partial\hat\sigma}\right], \tag{38}$$

$$\langle\Delta T^2\rangle = \langle\Delta T^2\rangle_0 + \frac{\varepsilon}{1+\varepsilon}\left[\frac{\lambda-1}{\lambda}\delta_1(\lambda) + (1-c_{1,\Delta T^2})\right.$$
$$\left. \times \frac{\partial\langle\Delta T^2\rangle_0}{\partial\hat\mu} - \sigma c_{2,\Delta T^2}\frac{\partial\langle\Delta T^2\rangle_0}{\partial\hat\sigma}\right], \tag{39}$$

where the respective quantity of the unperturbed system is taken at the effective parameters given in Eq. (37). We

Table 1
Values of the parameters c_1 and c_2 that lead to an exact solution in the linear theory Eqs. (38) and (39)

λ	c_1	c_2
0	0	0
1	1	0
∞	μ	1

In these cases $c_1 = c_{1,T} = c_{1,\Delta T^2}$ and $c_2 = c_{2,T} = c_{2,\Delta T^2}$.

have added indices to the respective parameters c_1 and c_2, indicating that the values of these parameters may differ for mean and variance.

It can be proven (see Appendix A) that the values for c_1 and c_2 listed in Table 1 lead to the exact solution for mean and variance provided the decay rate has the corresponding value found in Table 1. In these special cases, the terms $\langle T\rangle_0$ and $\langle\Delta T^2\rangle_0$ give the exact solution and the linear correction vanishes. Thus given a value of the decay rate close to one of the special values in Table 1, we may use Eqs. (38) and (39) in order to calculate the first two central moments of the ISI.

We are, however, also interested in the general dependence of the ISI's mean and variance on λ. In this case, a reasonable choice for the parameters that does not lead to too cumbersome formulas is (see Appendix A)

$$c_{2,T} = c_{2,\Delta T^2} = 0, \tag{40}$$

$$c_{1,T} = 1 + \frac{\lambda-1}{\lambda}\frac{\delta_1(\lambda)}{\partial\langle T\rangle_0/\partial\mu}, \tag{41}$$

$$c_{1,\Delta T^2} = 1 + \frac{\lambda-1}{\lambda}\frac{\delta_2(\lambda)}{\partial\langle\Delta T^2\rangle_0/\partial\mu}. \tag{42}$$

Here all functions on the r.h.s. are taken at $\varepsilon = 0$. Hence, in order to calculate mean and variance, one must determine the parameters $c_{1,\Delta T^2}, c_{1,T}$ by means of Eqs. (41) and (42) and then use these values together with Eq. (40) in Eqs. (38) and (39). Note that these formulas reproduce the values of c_1 and c_2 found in Table 1 at $\lambda = 0$ and $\lambda = 1$ but not at $\lambda \to \infty$. While comparing to the results of the computer simulations, we will always use Eq. (38) or Eq. (39) with the parameters calculated by Eqs. (40), (41), and (42).

4. Discussion of the results; comparison to numerical simulations

Here we plot mean, variance, and CV of the ISI as functions of the decay rate λ. We also look at the firing rate and the CV as functions of input current and noise intensity. We compare a subset of the analytical curves

to simulation results which where obtained as explained in Section 2.1.

Before we proceed let us briefly explain how the time scales in our non-dimensional model are related to those of a real neuron. As pointed out in the introduction, time is measured in units of the membrane time constant τ_{mem} which is typically of the order $\tau_{mem} \sim 10$ ms. The dimensional decay rate of the threshold is thus obtained by dividing the non-dimensional rate λ by the membrane time constant. For $\tau_{mem} = 10$ ms, a low decay rate of $\lambda = 0.01$ would thus correspond in real time to a decay rate of 1 Hz. Further, when we talk about an ISI it is given in terms of τ_{mem}, e.g. if $\tau_{mem} = 10$ ms a non-dimensional mean ISI of 4 corresponds to a ISI of 40 ms in real time or to a firing rate of 25 Hz. In a similar way we obtain the variance in real time by multiplying the variance obtained from our model by τ_{mem}^2. Note that the CV being the *relative* standard deviation of the ISI does not depend on τ_{mem} and can thus be directly related to an experimentally measured CV.

4.1. Results for the perfect IF model

We choose $\mu = 1$ and a moderate noise intensity of $\sigma^2 = 0.2$ to study the dependence of the ISI's mean and variance on the decay rate of the threshold. Fig. 2 reveals a simple monotonous decrease of the mean with growing λ. The mean is also monotonously increased if we go to stronger amplitudes ε. One can easily check the limit cases of small and large decay rate: at $\lambda = 0$ the mean ISI approaches $(1 + \varepsilon)/\mu$, for large λ we obtain the value for the unperturbed system $1/\mu$. By plotting the deterministic ISI (Eq. (21)) linearized in ε) for comparison (thin dashed lines in Fig. 2), we see what the effect of the finite noise intensity is, namely, a fairly

weak one: only at large values of λ a finite noise results in a stronger modification of the mean ISI. In general, for weak up to moderate noise intensity, the expression for the deterministic mean ISI Eq. (21) will suffice to describe the effect of the threshold and cover even the range of larger amplitudes ε.

The theory given by Eq. (15) agrees fairly well with the simulation data up to an amplitude $\varepsilon = 0.1$. For $\varepsilon = 0.2$ the theory seems to slightly overestimate the effect of the time-dependent threshold for intermediate values of the decay rate. Changing the noise intensity does not change the range of validity of the linear approximation (not shown) (Fig. 3).

The variance of the ISI for the perfect IF model displays a more interesting dependence on the decay rate. First of all, it can be either smaller or larger than in the unperturbed case depending on the system's parameters (in particular on the decay rate). For large decay rate the variance tends to that of the unperturbed system ($\varepsilon = 0$). By decreasing the rate, the variance becomes smaller than for $\varepsilon = 0$. This can be understood as the effect of a quickly decaying threshold that suppresses at short times ($t < \langle T \rangle_0$) the occurrence of short ISIs. These short ISIs appear now at a later instant, most likely in the mode of the ISI density. In other words, probability at short ISIs is moved into the mode of the probability density, consequently the variance of this density will decrease. Upon further decreasing λ, the variance passes through a minimum, crosses the value of the unperturbed system and saturates finally at a value considerably larger than for $\varepsilon = 0$. Clearly, as we decrease λ, the threshold decay extends over longer and longer parts of the typical passage from $v = 0$ to $v = \Theta(t)$. If the decay time $1/\lambda$ gets equal to the mean ISI or even larger, the effect of moving short ISIs into the mode of the ISI density does not play a role anymore, but quite the
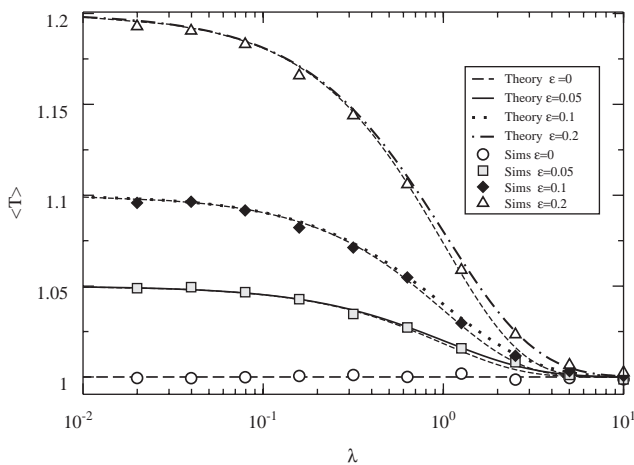

Fig. 2. The mean of the ISI vs. decay rate of the threshold for the perfect IF model. Simulations (symbols) and theory (lines) with the indicated values of the amplitude ε and $\sigma^2 = 0.2$. The thin dashed lines represent the linearized deterministic ISI for $\sigma = 0$ (first two terms of the second line in Eq. (21)).
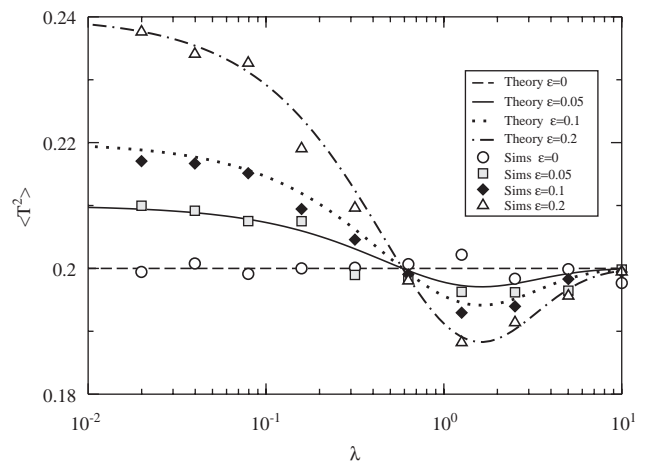

Fig. 3. The variance of the ISI vs. decay rate of the threshold for the perfect IF model. Simulations (symbols) and theory (lines) with the indicated values of the amplitude ε and $\sigma^2 = 0.2$.

contrary effect can be observed: realizations around the mode of the density will be shifted further out and hence the variance of the density will even increase compared to the unperturbed case $\varepsilon = 0$.

As a matter of fact, the variance displays a minimum only for sufficiently small noise intensity satisfying the condition

$$CV_0 = \sigma/\sqrt{\mu} < \sqrt{2} \tag{43}$$

as can be shown by inspecting Eq. (15). Furthermore, the decay rate which minimizes the variance can be expressed by the squared coefficient of variation, for brevity denoted by $R = CV^2$, and by the mean ISI of the unperturbed system $\langle T \rangle_0$

$$\lambda_{min} = \frac{\sqrt{1 + 4R - 2R^2} - 3R^2/2 + 4R - 1}{\langle T \rangle_0 R(2-R)^2}. \tag{44}$$

In the weak noise limit ($\sigma \to 0$), this value tends to

$$\lambda_{min} \to \frac{3}{2} \frac{1}{\langle T \rangle_0} \quad \text{as} \quad CV_0 \to 0. \tag{45}$$
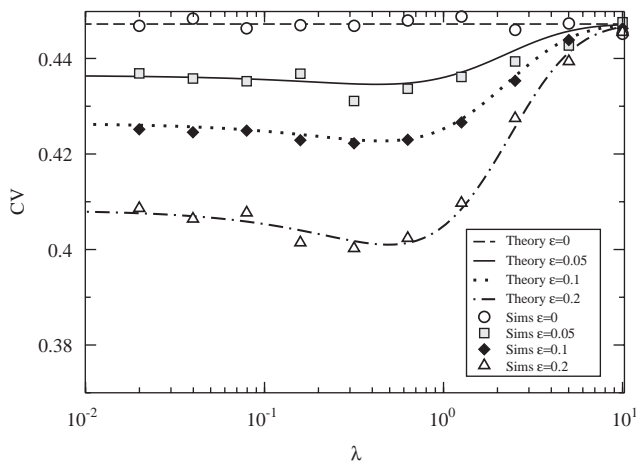

Fig. 4. The CV of the ISI vs. decay rate of the threshold for the perfect IF model. Simulations (symbols) and theory (lines) with the indicated values of the amplitude ε and $\sigma^2 = 0.2$.

For finite noise intensity, λ_{min} will be larger than this value (as long as condition Eq. (43) is met). The latter three relations are also found for an exponentially forced linear dynamics (Lindner, 2004b)—we recall that the variances in these two cases, i.e. Eqs. (14) and (16)) considered as functions of λ differ only by a constant.

Interestingly, although the variance can be either smaller or larger than in the case of a constant threshold, the relative variability as measured by the CV of the system with decaying threshold is always smaller than that for $\varepsilon = 0$ (cf. Fig. 4). Hence, the increase of the mean is stronger at low λ than the increase of the standard deviation. The CV attains a minimum for $\lambda \approx 0.5/\langle T \rangle_0$, i.e. if λ equals half of the firing rate of the unperturbed system. Further exploration reveals that this changes only slightly if base current or noise intensity are changed: the decay rate at which the minimum is attained varies between $0.5/\langle T \rangle_0$ (for weaker amplitude ε) and $1/\langle T \rangle_0$ (for stronger amplitude ε). The minimum does also occur for parameters at which the variance does not attain a minimum vs. λ. Thus, in general the time-dependent threshold leads to the strongest decrease of the relative variability if threshold decay and unperturbed firing of the perfect IF model have similar time scales.

Up to this point, we have considered the central moments of the ISI vs. the decay rate of the threshold, a picture that is convenient from the modelers point of view but hardly measurable in a real neuron. More common are plots of the transfer function, i.e. the relation between the constant base current μ and the output rate, shown in Fig. 5 (l.h.s.). We also plot the CV as a function of μ (Fig. 5, r.h.s.). In both figures, a stronger amplitude ($\varepsilon = 0.5$) is used to show more clearly the effect of the time-dependent threshold.

The rate of a perfect IF model with constant threshold is a simple linear function (it is zero for $\mu \leqslant 0$). From Fig. 5 it is seen that the input current at which the rate deviates from the linear behavior depends strongly on the decay rate. If the input current μ is sufficiently strong such that $\mu^2 \gg \lambda \sigma^2$ (this is the case for almost the entire
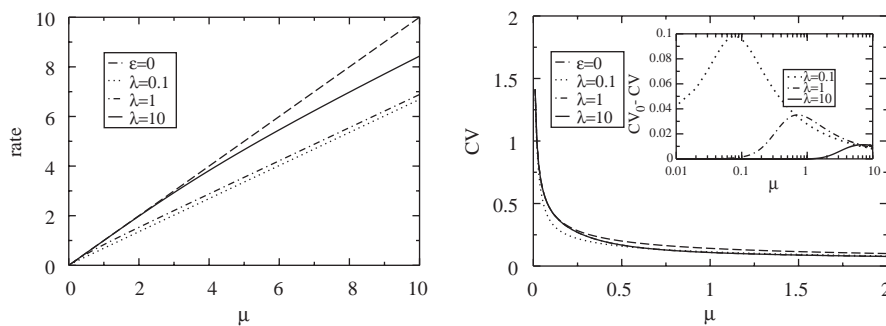

Fig. 5. Rate and CV of the ISI vs. input current μ for the perfect IF model. Theory Eqs. (15) and (3) with the indicated values of the decay rate λ. Other parameters: $\varepsilon = 0.5$ and $\sigma^2 = 0.2$.

range of μ shown in Fig. 5 (l.h.s.)), we can approximate the rate using Eq. (15) as follows:

$$r = \mu(1 + \varepsilon e^{-\lambda/\mu})^{-1}. \qquad (46)$$

With increasing μ this simple relation shows a turnover from $r \approx \mu$ (unperturbed system) to $r \approx \mu/(1 + \varepsilon)$ (unperturbed system with larger threshold $1 + \varepsilon$). The turning point depends only on λ but not on σ.

The CV is shown in Fig. 5 (r.h.s.). It decreases monotonously with increasing μ for all values of the decay rate. Remarkably, the difference between the CV for $\varepsilon = 0$ and the CV of the system with time-dependent threshold (inset) goes through a maximum. Put differently, the effect of the time-dependent threshold on the relative variability is maximal for a certain input current μ. The value of μ where the difference reaches its maximum is to a good approximation given by the base current that yields for $\varepsilon = 0$ a firing rate equal to 0.75λ. At the first glance this resembles the other condition we found for the minimum in the CV vs. λ where the decay rate had to be slightly *below* the firing rate of the

unperturbed system. To clarify the small quantitative discrepancy between the two conditions, we show in Fig. 6 the difference between the CVs of the perfect IF model without and with time-dependent threshold.

Clearly maxima are seen vs. λ as well as vs. μ, however, these do not correspond to one global maximum of the CV's difference. For $\lambda \approx 1$ (i.e. $\log(\lambda) \approx 0$), for instance, a maximum vs. μ is attained at a small base current. At this value of μ the difference in CVs can be further increased by decreasing the decay rate λ. Although maxima vs. λ and vs. μ are located at parameters that correspond to different ratios of decay rate and firing rate, we can state that *qualitatively* a time-scale matching condition is present: if the firing rate of the unperturbed system and the decay rate are of the *same order of magnitude* the effect of the time-dependent threshold on the relative variability of the ISI sequence will be strongest.

Fig. 7 shows rate and CV as functions of the noise intensity σ for different values of the decay rate λ. The rate dependence in the left panel illustrates nicely the validity of the simple expression given in Eq. (46), that is for $\sigma < 0.4$, the rate does not depend on the noise intensity at all. In the strong noise limit, we obtain the simple expression for the rate $\mu/(1 + \varepsilon)$, i.e. the rate saturates at the value given by a static increase of the threshold by ε.

The CV in turn increases linearly with growing noise intensity like the CV of the unperturbed system ($\varepsilon = 0$). The effect of the time-dependent threshold is mainly a simple offset of the CV compared to the unperturbed case. The difference between unperturbed and perturbed CV grows monotonously with σ, i.e. it does not show a maximum in contrast to Fig. 5 (inset in right panel) where we varied the input current μ instead of σ.

In conclusion, the exponentially decaying threshold in a perfect IF model results in an decreased relative ISI variability, in a enlargement of the mean ISI (decrease in firing rate), and in a variance (absolute variability) that can be larger (for small λ) or smaller (for large λ) than in the absence of the time-dependent threshold. $F - I$
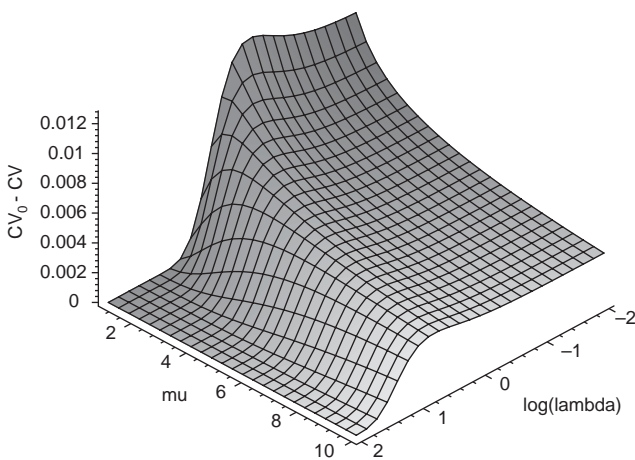

Fig. 6. Difference between CV for $\varepsilon = 0$ and $\varepsilon = 0.1$ vs. decay rate λ and input current μ for the perfect IF model. The decay rate is plotted logarithmically; the noise intensity is $\sigma^2 = 0.2$.
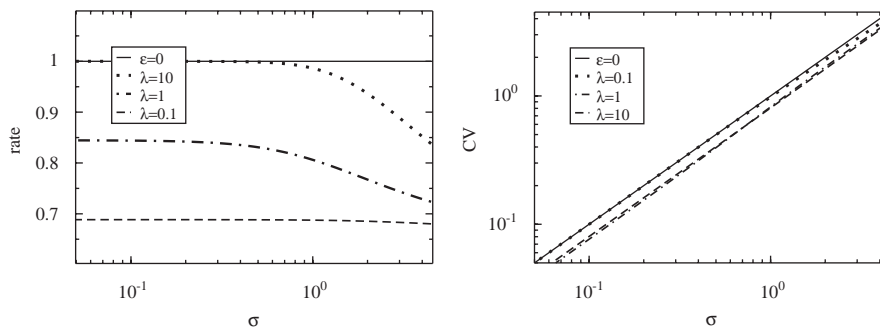

Fig. 7. Rate and CV of the ISI vs. noise intensity σ for the perfect IF model. Theory Eqs. (15) and (3) with the indicated values of the decay rate λ. Other parameters: $\varepsilon = 0.5$ and $\mu = 1$.

curves deviate slightly from the linear behavior of the standard perfect IF model, showing a simple turnover from the unperturbed case (at small input current) to the rate of the standard model with static threshold at $1 + \varepsilon$. The effect of the time-dependent threshold on the relative variability is minimized at a decay rate or a base current at which a time-scale matching condition is met: in this case the decay rate is equal to the rate of the unperturbed system. This condition resembles the effects of stochastic resonance (see Gammaitoni et al., 1998 for a review); the minimum in the CV in turn is also observed in another noise-induced effect: coherence resonance (Pikovsky and Kurths, 1997). Note, however, two important differences of our findings to the aforementioned noise-induced effects: (1) in our case the minimum in the CV is observed while varying decay rate or input current but not by varying the noise intensity; (2) there are no potential barriers or true excitability involved here, yet they are essential for the effects of stochastic resonance and coherence resonance.

4.2. Results for the leaky IF model

For the leaky IF model (with $\alpha = 1$ in Eq. (1)) we choose in the following a base current that is subthreshold ($\mu < 1$). In this case the firing statistics are significantly different from that of the perfect IF model and a qualitatively different behavior of rate and CV with respect to a variation of input current and noise intensity can be expected.

We first consider the mean, variance and CV as functions of the decay rate for $\mu = 0.8$ and a moderate noise intensity with $\sigma^2 = 0.2$. The value of the base current μ implies that the neuron is in the subthreshold or noise-induced firing regime in which the voltage can reach the threshold even in the unperturbed case $\varepsilon = 0$ only by the assistance of noise. Further, at these parameter values the firing is determined by two different, statistically independent processes: the passage of the voltage from the reset voltage $v = 0$ into the resting voltage $v = \mu$ (relaxation process) and the escape from the resting voltage to the time-dependent threshold (escape process). It is important to note that the escape process can only be realized in the presence of noise.

The mean ISI shown in Fig. 8 is a monotonously decreasing function of the decay rate like in the case of the perfect IF model. The approximation resulting from the optimized perturbation calculation reproduces the simulation data well up to an amplitude $\varepsilon = 0.1$; for $\varepsilon = 0.2$ we note that the real ISI is slightly underestimated by the analytical result.

The variance (Fig. 9) is almost always a decreasing function of the decay rate as well. A closer look at large decay rates (inset of Fig. 9) shows a small region where the variance undershoots that of the unperturbed system (i.e. that at $\lambda \to \infty$). This small decrease in absolute
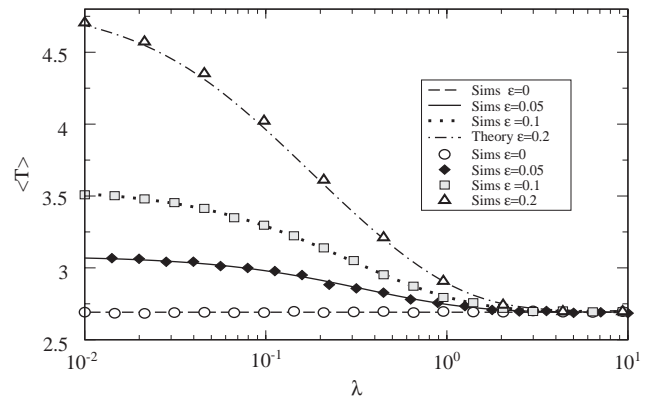

Fig. 8. The mean of the ISI vs. decay rate of the threshold for the leaky IF model. Simulations (symbols) and theory (lines) with the indicated values of the amplitude ε and $\sigma^2 = 0.2$.
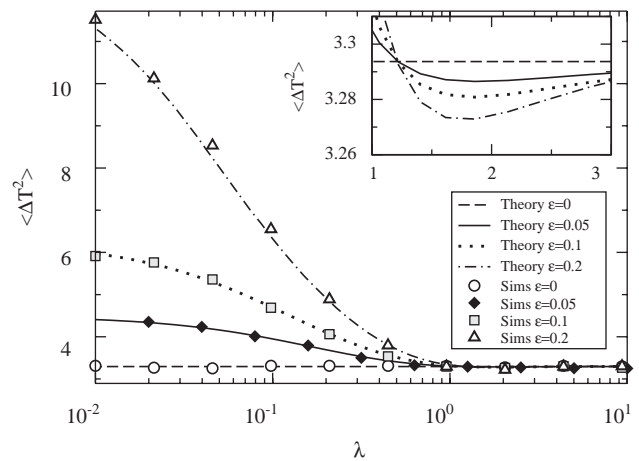

Fig. 9. The variance of the ISI vs. decay rate of the threshold for the leaky IF model. Simulations (symbols) and theory (lines) with the indicated values of the amplitude ε and $\sigma^2 = 0.2$.

variability is hard to verify by simulations and will therefore be also hardly observable in real neurons.

Once more, the picture is different if we consider the relative variability, that is the CV vs. decay rate (Fig. 10). The relative variability is considerably decreased (more than in the case of the perfect IF model, cf. Fig. 4) as long as the decay rate is in a certain range of moderate values. Below the lower limit of this range (≈ 0.04 with slight differences among curves for different values of ε), we find that the CV can be higher than in the unperturbed system which stands in marked contrast to the findings for the perfect IF model. In the limit $\lambda \to 0$ we deal with a constant, though increased threshold $1 + \varepsilon$. Why does this increased threshold lead to a higher relative variability? This can be understood by considering the independent processes of relaxation and escape the sum of which forms the entire first passage process as explained above. At low λ, the quasi

static increase of the threshold will increase the relative strength of the escape time while leaving the relaxation process (passage from zero to resting voltage) unchanged. Consequently, the entire process becomes more irregular, which becomes apparent by the high value of the CV at low λ. Following this line of reasoning it is also clear why this effect is not observed

in the perfect IF model where the escape time part of the ISI is absent (there is no potential barrier for the perfect IF model).

Next we discuss the dependence of spike rate and CV as functions of the input current μ and the noise intensity σ at different values of the decay rate λ. The transfer function (rate vs. input current) does not change compared to the unperturbed case if the decay rate is high ($\lambda = 10$). Deviations are present for $\lambda = 1$ and even more pronounced for $\lambda = 0.1$; the threshold decay in this case diminishes the slope of the transfer function.

The CV as a function of the input current decreases monotonously for all decay rates shown in Fig. 11 (r.h.s.). As for the transfer function, a threshold decay $\lambda = 10$ does not have much effect. For $\lambda = 1$ and $\lambda = 0.1$ the CV is decreased by the time-dependent threshold; this decrease is again maximal for a certain finite input current (cf. inset of Fig. 11, r.h.s.) which depends on the decay rate λ. Like in the case of the perfect IF model, the maximum is attained at an input current for which the rate of the unperturbed system is of the order of magnitude of the decay rate; in particular for the parameters used in Fig. 11 (r.h.s.), we have that $r_0(\mu_{max}) \approx 0.6\lambda$ for both $\lambda = 1$ and $\lambda = 0.1$.

The effect of the decaying threshold on the rate and the CV as functions of the noise intensity is shown in Fig. 12. Clearly, the smaller the decay rate, the larger the
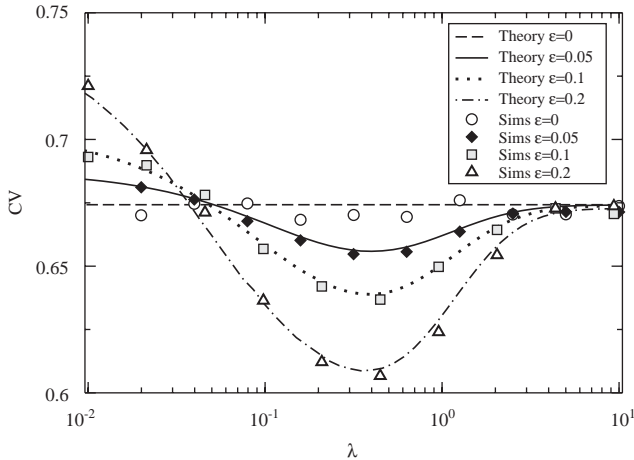

Fig. 10. The CV of the ISI vs. decay rate of the threshold for the leaky IF model. Simulations (symbols) and theory (lines) with the indicated values of the amplitude ε and $\sigma^2 = 0.2$.
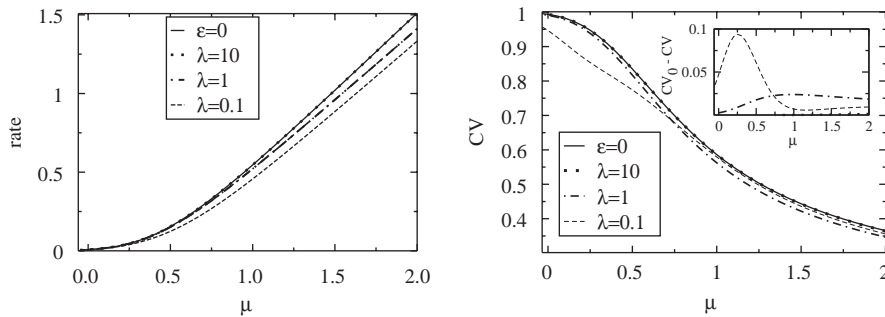

Fig. 11. Rate and CV of the ISI vs. input current μ for the leaky IF model. Theoretical results with the indicated values of the decay rate λ. Other parameters: $\varepsilon = 0.1$ and $\sigma^2 = 0.2$.
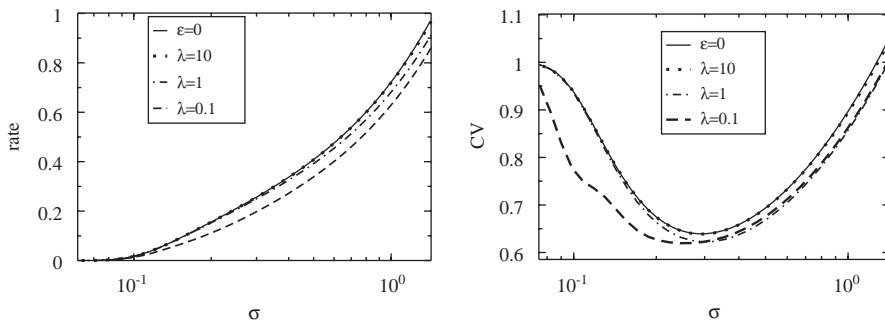

Fig. 12. Rate and CV of the ISI vs. noise intensity σ for the leaky IF model. Theoretical results with the indicated values of the decay rate λ. Other parameters: $\varepsilon = 0.1$ and $\mu = 0.8$.

effect on both rate and CV. Again for $\lambda = 10$, there is no appreciable effect of the threshold decay on the characteristic curves. For $\lambda = 0.1$ and $\lambda = 1$, the rate drops compared to the unperturbed case; the decrease is strongest at large noise intensity. For the CV in turn, the value of the decay rate determines strongly whether the effect of threshold decay is strongest at small or at large noise intensity. The CV shows a minimum vs. σ even in the case of a constant threshold ($\varepsilon = 0$). This is a manifestation of coherence resonance (Pikovsky and Kurths, 1997) and has been found previously in the leaky IF model with constant threshold (Pakdaman et al., 2001; Lindner et al., 2002). It is a consequence of the different dependences of the relaxation and escape processes on the noise intensity. As we see in Fig. 12 (r.h.s.), a time dependent threshold with decay rate $\lambda = 1$ decreases the CV around the minimum and also at larger noise intensities; its effect vanishes in the weak noise limit. This is qualitatively different if we consider the slower decay of the threshold with $\lambda = 0.1$. Still the minimum of the CV is deepened though not as strongly as for $\lambda = 1$. Most importantly, the strongest deviation is obtained at fairly small noise where the CV of the unperturbed system is already close to one which is the Poisson limit. We note that the same limit is actually approached if we decrease the input current μ sufficiently. Therefore, the strongest impact of the threshold decay on the relative variability at $\lambda = 0.1$ for both the CV vs. μ and the CV vs. σ occurs if the leaky IF model operates in a Poissonian firing regime with a time-dependent rate.

We note that the decrease of the CV at small base current or small noise intensity for $\lambda = 0.1$ is so strong that it should be taken with caution (the theory is actually only valid as long as the statistics are changed only slightly). The strong effect of a threshold decay with $\lambda = 0.1$ variability raises the question of what is going to happen if we go to even smaller decay rates. In Fig. 13 we show the CV vs. μ (l.h.s.) and vs. σ (r.h.s.) for $\lambda = 0.01$. Here a qualitative change of these curves can

be observed: the CV goes through a minimum upon varying μ as well as σ in a parameter range where the leaky IF with constant threshold generates a Poisson spike train. Minima are predicted by the theory in both cases and confirmed by the results of computer simulations. However, we note that the theory based on a linear correction is not very good just around the parameter values that minimize the CV; in fact, the theory breaks down (yielding negative "variance" and the like) for the largest amplitude $\varepsilon = 0.05$ in Fig. 13 (r.h.s.). This is to be expected since the linear correction cannot be good at providing large corrections to the unperturbed case as they are seen in the results of the simulations.

The origin of the new minimum occurring in the Poissonian parameter regime becomes clear by realizing that the minimum appears at parameters for which the firing rate is of the same order of magnitude like the decay rate. At much lower input current or noise intensity, the mean interval is much larger and thus only a small fraction of realizations is influenced by the threshold decay; most realizations "see" a constant threshold and hence in this limit the CV tends to one. On the other hand, beyond the respective "optimal" value of μ or σ the threshold decay starts to look slow, most realizations will pass the threshold before it has appreciably changed; also in this case the irregularity will tend to that of the Poisson process. The reason that the Poisson limit is actually *not* approached in this case is evident: going beyond small base current and small noise intensities brings all the internal dynamics into play, again.

Certainly, the minimum in the CV seen while varying externally controllable parameters like input current or input noise is the most pronounced manifestation of the threshold decay. Such minima have been actually observed experimentally (Goldberg et al., 1984) and in other models (Smith and Goldberg, 1986) although not in the Poissonian firing regime but for regularly firing neurons. The dynamical mechanism thus seems to be quite different from the one observed here.
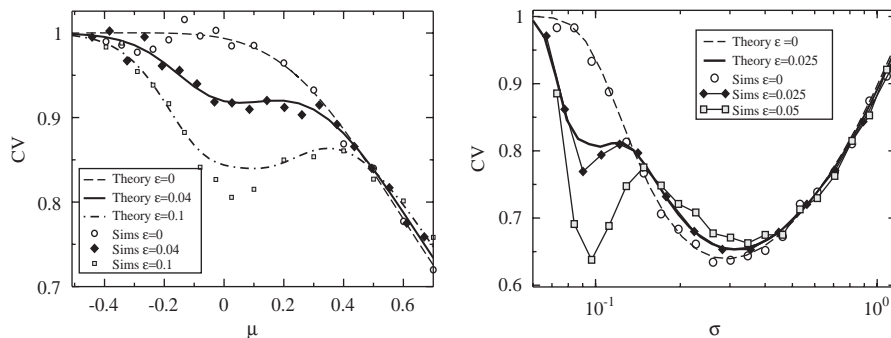

Fig. 13. CV of the ISI vs. input current μ (left) and noise intensity σ (right) for the leaky IF model at $\lambda = 0.01$. Theoretical results with the indicated values of the amplitude ε (theory is not plotted for $\varepsilon = 0.05$ in the right panel, see text). Other parameters: $\sigma^2 = 0.2$ (left panel) and $\mu = 0.8$ (right panel). Because of the low spike rate at small noise we used a smaller number of ISIs than our standard value $N = 10^6$ but at least $N = 10^4$ ISIs.

5. Summary and conclusions

In this paper, we have studied the effect of an exponentially decaying threshold on the ISI statistics for both perfect and leaky IF models driven by white Gaussian noise.

In the case of the perfect IF model, we have shown that the mean ISI is generally slightly increased while the variance can be either increased (at low decay rates) or decreased (at large decay rates) due to the threshold decay. The variance attains a minimum for a decay rate that is of the same order of magnitude as the firing rate of the neuron. Remarkably, the CV which quantifies the relative variability is, however, always smaller than for a constant threshold. In this sense, the exponentially decaying threshold introduces an additional relative refractory period into the dynamics of a perfect IF model. We furthermore demonstrated that the transfer function shows a turnover between two linear curves with increasing input (or base) current. Varying the input current we also found that the effect of the threshold decay on the CV is maximized if the firing rate of the neuron matches the decay rate of the threshold. It is important to note, however, that all of these effects are comparably weak: a 20% change in the threshold amplitude yields only a change of the CV by a small fraction.

For the leaky IF model, we found an increase in both mean and variance of the ISI; only a very small decrease of the variance was seen at large decay rates of the threshold. The CV is in this case reduced for moderate up to large decay rates; an increase of the CV at low decay rates could be explained by the effect of an increased quasi-static threshold for low decay rates. The influence of the decaying threshold on the transfer function is—as in the case of the perfect IF model—fairly weak. Considering the CV as a function of base current or noise intensity we uncovered an interesting effect at low decay rate. In a regime at low base current or small noise intensity, the CV shows a minimum whenever the firing rate is of the same order of magnitude as the decay rate. The minimum can be considerably deeper than the CV for constant threshold (which is about one) already for amplitudes of the decaying threshold that have in all other parameter regimes a negligible effect on the ISI statistics. We note that considering the CV vs. noise intensity, the novel minimum is observed at much lower noise intensity than the well-known coherence-resonance minimum.

The calculation of the ISI's mean and variance presented in this paper can be regarded as a first step for the analytical treatment of the non-renewal LIFDT model mentioned in the introduction. In the latter model, the threshold decays exponentially like in our model; the threshold is, however, increased by a constant A whenever the neuron fires instead of being reset to a fixed value. Consequently, the initial value of the threshold $1 + \varepsilon_i$ will be a random variable depending on the spike history. For a fixed value of ε_i we can use the formulas for mean and variance derived in this paper; the random nature of the initial value ε_i then requires an additional average that is beyond the framework of the present paper. It is, however, not too hard to see that for small jump amplitude A we have $\varepsilon_i \sim A$; in this case, the corrections to the mean and variance will only depend on the *mean value* of the initial value of the threshold $\langle \varepsilon_i \rangle$. Therefore, at fixed system parameters, the mean and variance of the LIFDT model equal those of a renewal leaky IF model with decaying threshold with an effective amplitude $\langle \varepsilon_i \rangle$.

The reduction in rate and CV demonstrated for both the perfect and leaky IF models, may have an effect on the neural signal transmission. The reduction in rate will certainly diminish the susceptibility of the neuron, i.e. its spectral sensitivity with respect to a weak time-dependent modulation of the input current. It will, however, also strongly reduce the noise floor since, at low frequencies, this is given by the product $CV^2 r$ (Cox and Lewis, 1966). Which of these effects is stronger in affecting the spectral signal-to-noise ratio will certainly depend on the model and its parameters; this remains an interesting questions for a future investigation.

Appendix A. Optimizing the perturbation result for the leaky IF model

Here we first show that if λ takes on one of the specific values in Table 1, Eqs. (38) and (39) with the values of c_1 and c_2 taken from Table 1 will lead to exact solutions for mean and variance of the ISI. Furthermore, we derive the formulas for c_1 Eqs. (41) and (42) that give a good approximation for the respective quantities ($\langle T \rangle$ or $\langle \Delta T^2 \rangle$) for an arbitrary value of λ.

As a matter of fact, for the leaky IF model with constant threshold and drift term, each moment and also every function of the moments (e.g. the variance) can be written as a function of two effective parameters $f(x_1, x_2)$ with

$$x_1 = \frac{\mu - v_T}{\sigma}, \quad x_2 = \frac{\mu - v_R}{\sigma}, \tag{47}$$

where v_T and v_R are constant (but arbitrary) threshold and reset voltages, respectively. This follows readily from the fact that the Laplace transform of the ISI density $\rho_0(\lambda)$ (see Eq. (31)) from which the moments can be derived does only depend on these two parameters.

Next, we rewrite Eqs. (38) and (39) in the general form

$$F = f\left(x_1 = \frac{\mu + \varepsilon c_1 - (1 + \varepsilon)}{\sigma(1 + \varepsilon c_2)}, x_2 = \frac{\mu + \varepsilon c_1}{\sigma(1 + \varepsilon c_2)}\right)$$
$$+ \frac{\varepsilon}{1 + \varepsilon}\left[\frac{\lambda - 1}{\lambda}\delta_f(\lambda) + (1 - c_1)\frac{\partial f}{\partial \hat{\mu}} - \sigma c_2 \frac{\partial f}{\partial \hat{\sigma}}\right]. \quad (48)$$

Here F denotes either mean or variance, f is the respective quantity in the unperturbed case, and $\delta_f(\lambda)$ stands for the linear correction due to the time-dependent drift.

The exact solutions for F at $\lambda = 0$ and ∞ and at $\lambda = 1$ can be inferred from the rescaled parameters of the standard leaky IF in Eqs. (1), (2), and (22), respectively

$$F = f\left(x_1 = \frac{\mu - (1 + \varepsilon)}{\sigma}, x_2 = \frac{\mu}{\sigma}\right), \quad \lambda = 0, \quad (49)$$

$$F = f\left(x_1 = \frac{(\mu + \varepsilon)/(1 + \varepsilon) - 1}{\sigma/(1 + \varepsilon)}, x_2 = \frac{(\mu + \varepsilon)/(1 + \varepsilon)}{\sigma/(1 + \varepsilon)}\right)$$
$$= f\left(x_1 = \frac{\mu - 1}{\sigma}, x_2 = \frac{(\mu - (-\varepsilon))}{\sigma}\right), \quad \lambda = 1, \quad (50)$$

$$F = f\left(x_1 = \frac{\mu - 1}{\sigma}, x_2 = \frac{\mu}{\sigma}\right). \quad \lambda \to \infty. \quad (51)$$

In words: (i) for $\lambda = 0$, the function F corresponds to the function with constant threshold and constant drift but with a threshold $v_T = 1 + \varepsilon$; (ii) for $\lambda = 1$, F corresponds to the unperturbed system with an reset point at $v_R = -\varepsilon$; (iii) for $\lambda \to \infty$, the function F is equal to that of the standard leaky IF, namely f with standard parameters.

Comparing the values of x_1 and x_2 in the first term of Eq. (48) to those in Eqs. (49)–(51), we can solve for c_1 and c_2 and find the values that are displayed in Table 1. Next we show that for a parameter set taken from Table 1, the second term in Eq. (48) (the linear correction) vanishes.

For $\lambda = 0, c_1 = 0$, and $c_2 = 0$ the exponential forcing turns into a static forcing, implying that the linear correction with respect to the time-dependent drift must approach the linear correction with respect to a static change of the base current multiplied by the decay rate

$$\delta_f(\lambda) \to \lambda \frac{\partial f}{\partial \hat{\mu}} \quad \text{as } \lambda \to 0, \quad (52)$$

which leads in Eq. (48) to

$$[\cdots]_{\lambda = 0} = -\frac{\partial f}{\partial \hat{\mu}} + \frac{\partial f}{\partial \hat{\mu}} = 0 \quad (53)$$

as asserted.

For $\lambda = 1$ and $c_1 = 1, c_2 = 0$ according to Table 1, all terms in the squared bracket vanish because of the vanishing prefactors. Thus also in this case the assertion holds true.

Finally, for $\lambda \to \infty$ the dynamical correction δ_f approaches the linear correction with respect to a static change in the initial point; recall that δ_f was the response to $\lambda \exp(-\lambda t)$ that tends for $\lambda \to \infty$ to a δ spike at $t = 0$. It is readily seen that the linear correction with respect to a change in the initial point can be expressed as follows according to Eq. (47) (note that we dropped the dependence on v_R in Eq. (48) by setting $v_R = 0$)

$$\lim_{\lambda \to \infty} \delta_f(\lambda) = \frac{\partial f}{\partial v_R} = -\frac{1}{\hat{\sigma}}\frac{\partial f}{\partial x_2}. \quad (54)$$

Expressing now the derivatives with respect to μ and σ as derivatives with respect to x_1 and x_2, we obtain with the values $c_1 = \mu$ and $c_2 = 1$, that $\hat{\mu} = \mu$ and $\hat{\sigma} = \sigma$. The second term in Eq. (48) reads now

$$[\cdots]_{\lambda \to \infty} \to -\frac{1}{\sigma}\frac{\partial f}{\partial x_2} + \frac{1 - \mu}{\sigma}\left(\frac{\partial f}{\partial x_1} + \frac{\partial f}{\partial x_2}\right)$$
$$+ \frac{1}{\sigma}\left((\mu - 1)\frac{\partial f}{\partial x_1} + \mu\frac{\partial f}{\partial x_2}\right) = 0 \quad (55)$$

as asserted.

After having shown that the values of c_1 and c_2 in the Table 1 lead to the exact results at the specific values of λ, we turn now to the question of how c_1 and c_2 should be chosen if λ is arbitrary. Note first that the values in Table 1 have in common that the linear correction (the square bracket in Eq. (48)) vanishes. For an arbitrary value of λ, it is thus reasonable to demand that the absolute value of the linear correction should be minimized with respect to c_1 and c_2. To simplify the matter we require furthermore that (i) $c_2 = 0$ (corresponding to the optimized values of c_2 at $\lambda = 0$ and $\lambda = 1$) and (ii) the value c_1 does not depend on the amplitude ε. We note that an optimization with respect to c_1 and c_2 is possible; the resulting formulas are, however, not unique (there are two different solutions for small λ each of which covers one of the exact solvable cases $\lambda = 0$ and $\lambda = 1$) and also too cumbersome to be of much practical use. If $c_2 = 0$, we obtain from setting the square bracket in Eq. (48) to zero (which is obviously the minimum of the absolute value)

$$c_1 = 1 + \frac{(\lambda - 1)\delta_f}{\lambda \partial f/\partial \hat{\mu}}. \quad (56)$$

In general, also the right-hand side of this equation does depend on c_1 and also on ε through the effective parameter $\hat{\mu}$. The condition that c_1 should be independent of ε then leads to the simple conclusion to take the r.h.s. of Eq. (56) at vanishing amplitude. With this we obtain Eqs. (41) and (42).

Finally, we show in Fig. 14 the CV for the leaky IF model vs. decay rate λ in order to illustrate the different approximations discussed above. The line corresponding to the optimized values of $c_{1,T}$ and $c_{1,\Delta T^2}$ (which are functions of λ, μ and σ) describes reasonably well the simulation data. This is even the case for large λ where the approximation does not reproduce the exact result (here the dotted line for $c_1 = \mu$ and $c_2 = 1$ gives the correct result). Each of the approximations with pairs c_1
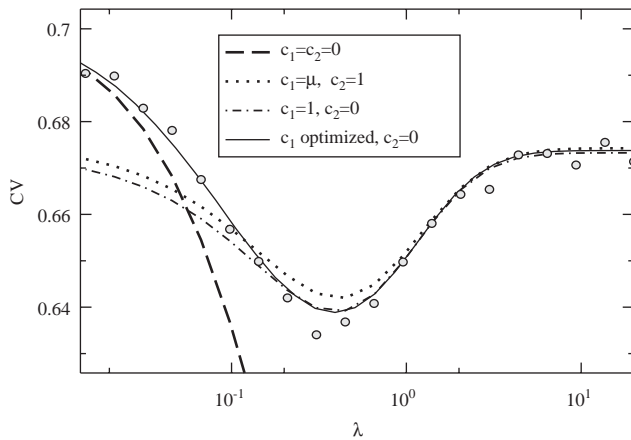
Fig. 14. The CV of the ISI vs. decay rate of the threshold for the leaky IF model. Simulations (symbols) and different theoretical results (lines) with the indicated values of c_1 and c_2. Other parameters: $\mu = 0.8, \varepsilon = 0.1, \sigma^2 = 0.2$.

and c_2 taken from Table 1 reproduces the data for values of λ close to the respective special value from Table 1. While the approximations resulting from $c_1 = 1, c_2 = 0$ and $c_1 = \mu, c_2 = 1$ deviate significantly only for small decay rate λ, the approximation $c_1 = c_2 = 0$ (dashed line) deviates strongly for all λ above a very small critical value ($\approx 10^{-1}$).

The formulas for mean and variance derived cover a large area in the parameter space, including moderate up to large noise intensity σ, small positive (subcritical) up to large (supracritical) base currents μ, and the entire range of decay rates. Caution must be used, however, in a specific parameter range. If the base current is subthreshold ($\mu < 1$), the decay of the threshold is slow ($\lambda \ll 1$), the formulas for mean and variance fail in the weak noise limit $\sigma \to 0$ in the sense that we have to choose smaller and smaller amplitude ε to achieve an agreement between theory and simulation results. The simple reason is that in this regime the dependence of the ISI moments on the time-dependent threshold becomes strongly nonlinear. To illustrate this consider the mean ISI in the small noise limit at a static threshold $v_T + \varepsilon$. If $\mu < 1$ the mean approaches asymptotically

$$\langle T \rangle \sim \exp\left[\frac{(v_T + \varepsilon)^2}{\sigma^2}\right] \tag{57}$$

and the ratio between perturbed and unperturbed mean becomes

$$\langle T \rangle / \langle T \rangle_0 \sim \exp\left[\frac{2\varepsilon v_T}{\sigma^2}\right], \tag{58}$$

where we have only taken into account the leading order in ε. It is easily seen from the latter relation that the ratio can become arbitrary large as we let $\sigma \to 0$, i.e. perturbed and unperturbed mean diverge exponentially and any perturbation calculation based on only a small difference between $\langle T \rangle$ and $\langle T \rangle_0$ must fail.

References

Abramowitz, M., Stegun, I.A., 1970. Handbook of Mathematical Functions. Dover, New York.

Brunel, N., Latham, P.E., 2003. Firing rate of the noisy quadratic integrate-and-fire neuron. Neural Comput. 15, 2281.

Chacron, M.J., Longtin, A., St-Hilaire, M., Maler, L., 2000. Suprathreshold stochastic firing dynamics with memory in P-type electroreceptors. Phys. Rev. Lett. 85, 1576.

Chacron, M.J., Longtin, A., Maler, L., 2001. Negative interspike interval correlations increase the neuronal capacity for encoding time-dependent stimuli. J. Neurosci. 21, 5328.

Chacron, M.J., Pakdaman, K., Longtin, A., 2003. Interspike interval correlations, memory, adaptation, and refractoriness in a leaky integrate-and-fire model with threshold fatigue. Neural Comput. 15, 253.

Corless, R.M., Gonnet, G.H., Hare, D.E.G., Jeffrey, D.J., Knuth, D.E., 1996. On the Lambert W function. Adv. Comput. Math. 5, 329.

Cox, D.R., Lewis, P.A.W., 1966. The Statistical Analysis of Series of Events. Chapman & Hall, London.

Ermentrout, G.B., 1996. Type I membranes, phase resetting curves, and synchrony. Neural. Comput. 8, 979.

Fourcaud, N., Brunel, N., 2002. Dynamics of the firing probability of noisy integrate-and-fire neurons. Neural Comput. 14, 2057.

Gammaitoni, L., Hänggi, P., Jung, P., Marchesoni, F., 1998. Stochastic resonance. Rev. Mod. Phys. 70, 223.

Giorno, V., Nobile, A.G., Ricciardi, L.M., 1990. On the asymptotic behaviour of first-passage-time densities for one-dimensional diffusion processes and varying boundaries. Adv. Appl. Probab. 22, 883.

Goldberg, J.M., Smith, C.E., Fernandez, C., 1984. The relation between discharge regularity and responses to externally applied galvanic currents in vestibular nerve afferents of the squirrel monkey. J. Neurophysiol. 51, 1236.

Gutiérrez, R., Ricciardi, L.M., Román, P., Torres, F., 1997. First-passage-time densities for time-non-homogeneous diffusion processes. J. Appl. Probab. 34, 623.

Gutkin, B.S., Ermentrout, G.B., 1998. Dynamics of membrane excitability determine interspike interval variability: A link between spike generation mechanisms and cortical spike train statistics. Neural Comput. 10, 1047.

Holden, A.V., 1976. Models of the Stochastic Activity of Neurones. Springer, Berlin.

Honerkamp, J., 1993. Stochastic Dynamical Systems. Concepts, Numerical Methods, Data Analysis. Wiley/VCH, Weinheim.

Jáimez, R.G., Román Román, P., TorresRuiz, F., 1995. A note on the Volterra integral equation for the first-passage-time probability density. J. Appl. Probab. 32, 635.

Lánský, P., Rospars, J.P., 1995. Ornstein–Uhlenbeck model neuron revisited. Biol. Cybernet. 72, 397.

Lindner, B., 2004a. Interspike interval statistics of neurons driven by colored noise. Phys. Rev. E 69, 022901.

Lindner, B., 2004b. Moments of the first passage time under weak external driving. J. Stat. Phys., in press, see also arXiv:cond–mat/0312017.

Lindner, B., Schimansky-Geier, L., Longtin, A., 2002. Maximizing spike train coherence or incoherence in the leaky integrate-and-fire model. Phys. Rev. E 66, 031916.

Lindner, B., Longtin, A., Bulsara, A., 2003. Analytic expressions for rate and CV of a type I neuron driven by white Gaussian noise. Neural Comput. 15, 1761.

Middleton, J.W., Chacron, M., Lindner, B., Longtin, A., 2003. Firing statistics of a neuron model driven by long-range correlated noise. Phys. Rev. E 68, 021920.

Pakdaman, K., Tanabe, S., Shimokawa, T., 2001. Coherence resonance and discharge reliability in neurons and neuronal models. Neural Networks 14, 895.

Pikovsky, A., Kurths, J., 1997. Coherence resonance in a noise-driven excitable system. Phys. Rev. Lett. 78, 775.

Rappel, W.-J., Karma, A., 1996. Noise-induced coherence in neural networks. Phys. Rev. Lett. 77, 3256.

Ricciardi, L.M., Sacerdote, L., 1979. The Ornstein–Uhlenbeck process as a model for neuronal activity. Biol. Cybernet. 35, 1.

Risken, H., 1984. The Fokker–Planck Equation. Springer, Berlin.

Smith, C.E., Goldberg, J.M., 1986. A stochastic hyperpolarization model of repetitive activity in vestibular afferents. Biol. Cybernet. 54, 41.

Tuckwell, H.C., 1978. Recurrent inhibition and afterhyperpolarization: Effects on neuronal discharge. Biol. Cybernet. 30, 115.

Tuckwell, H.C., 1988. Introduction to Theoretical Neurobiology. Cambridge University Press, Cambridge.

Tuckwell, H.C., Wan, F.Y.M., 1984. First passage time of Markov processes to moving barriers. J. Appl. Probab. 21, 695.

Vasudevan, R., Vittal, P.R., 1982. Time-dependent barriers and first-passage times-different types of neuronal models. Neurol. Res. 4, 63.

Wilbur, W., Rinzel, J., 1983. A theoretical basis for large coefficient of variation and bimodality in neuronal interspike interval distributions. J. Theor. Biol. 105, 345.